Water Research 290 (2026) 125060

Contents lists available at ScienceDirect

Water Research

journal homepage: www.elsevier.com/locate/watres

New insights into machine learning prediction techniques for real-time sanitary risk assessment in karst drinking water sources affected by faecal contamination

Jaime Fernández-Ortega *, Juan Antonio Barberá, Bartolomé Andreo

Department of Geology and Centre of Hydrogeology (CEHIUMA), Ada Byron Research Building, University of Malaga 29071 Malaga, Spain

HIGHLIGHTS

- First study to use ML for real-time sanitary risk assessment in karst groundwater.
- The method overcomes time and budget limitations of traditional bacterial cultures.
- Site-specific water parameters and ML models are required for a proper system analysis.
- Suitable for early-warning strategies on a wide range of drinking water supply schemes.

GRAPHICAL ABSTRACT

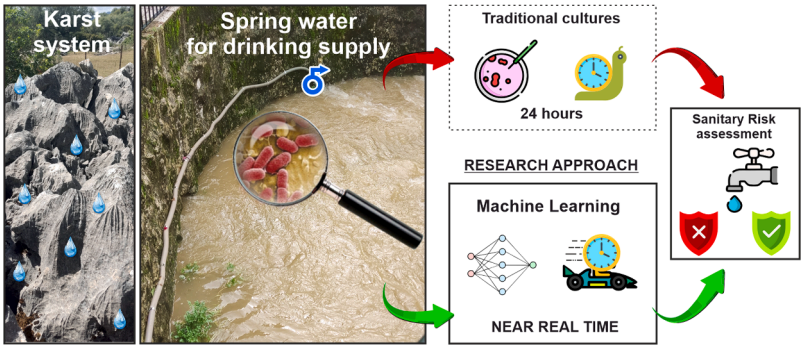

ARTICLE INFO

Keywords:
Karst groundwater
Drinking water
Faecal contamination
Early-warning
Southern spain

ABSTRACT

Safe drinking water supply from karst aquifers faces several challenges due to their high vulnerability to contamination, which can result in abrupt water quality variations in matter of hours. The analysis of faecal bacterial activity requires time-consuming cultures and expensive reagents in the laboratory, which can delay the detection of an imminent contamination event. An innovative methodology is proposed in this research to overcome these limitations and provide real-time insights about water quality in drinking sources. Fieldwork activities included the continuous monitoring of water parameters (spring discharge, electrical conductivity, turbidity and Tryptophan-like fluorescence) and groundwater sampling for *Escherichia coli* determination in two springs draining a binary karst aquifer in S Spain during three hydrological years (2020/21 to 2022/23). Ten supervised Machine Learning models were then tested to infer five sanitary risk levels (based on *E. coli* activity) from continuous measurements at the springs. The combination of two water parameters was the most effective predictor at the two drinking water sources, which showed different optimal configuration of proxy parameters depending on their hydrogeological features and contaminant transport mechanisms. Gaussian Processes, Neural Networks, Naïve Bayes and Quadratic Discriminant Analysis provided the highest probability of correctly discriminating between sanitary risk levels. This methodology holds significant potential to be integrated as an early-warning protection tool for real-time sanitary risk assessment and, thus, safeguarding drinking water supplies worldwide against microbial threats.

* Corresponding author.
E-mail address: jaimeortega@uma.es (J. Fernández-Ortega).

https://doi.org/10.1016/j.watres.2025.125060
Received 21 October 2025; Received in revised form 25 November 2025; Accepted 27 November 2025
Available online 29 November 2025

1. Introduction

Karst aquifers constitute a reliable source of drinking water and supply to approximately 678 million people, about 9.2 % of the world's population demand (Stevanovic, 2019). Due to their intrinsic characteristics (heterogeneous flow system through carbonate matrix, fractures and conduits), karst aquifers are highly vulnerable to contamination (Ford and Williams, 2007; Goldscheider and Drew, 2007). During precipitation events, high loadings of nutrients, sediments, and faecal materials from human activities may be flushed into the karst system via swallow holes, resulting in spring water contamination (Mahler et al., 2000; Pronk et al., 2007) and the interruption of urban supplies (Beaudeau et al., 2012).

Many pathogens of faecal origin, such as pathogenic strains of *Escherichia coli* (*E. coli*) are easily transported through water and might be responsible for human infections and other diseases (Ashbolt, 2004). The occasional contamination of groundwater systems in addition to standard water treatment processes, which are sometimes ineffective at removing all potential hazards (Onyango et al., 2015), suppose a direct risk for human health (WHO, 2006). Thus, abrupt and rapid (in a matter of hours) microbial activity variations in karst springs pose a significant hazard to water consumers supplied from this type of sources (Katz et al., 2011). A rapid (near real-time) assessment of water quality is then essential to avoid the potential public-health risks from waterborne diseases in karst terrains.

Within the framework of drinking water source protection, early warning systems (EWS) have been developed for the last 50 years to support decision-making processes and to reduce the potential risk to public health (U.S. EPA, 2005). These address the critical need to rapidly detect and respond to circumstances of accidental (or deliberate) contamination (Storey et al., 2011). However, the application of EWS in karst systems has received limited testing (Fernández-Ortega et al., 2024b; Frank et al., 2022; Grimmeisen et al., 2018; Ravbar et al., 2023; Stadler et al., 2010).

Given that conventional determination of faecal activity relies on labour-intensive, time-consuming and relatively expensive ($21 on average; Delaire et al., 2017) laboratory cultures, scientific efforts have primarily focused on pursuing groundwater parameters such as spring discharge (Auckenthaler et al., 2002), turbidity (Massei et al., 2003; Ryan and Meiman, 1996), particle size distribution (Pronk et al., 2007) or organic carbon (Frank et al., 2018) that may indirectly indicate the presence of potential contaminants at drinking water capture points. Recently, fluorescence spectrophotometry has emerged as a powerful tool for a quick and reliable detection of contamination-related parameters (e.g., turbidity or Tryptophan-Like-Fluorescence (TLF); Henderson et al., 2009; Hudson et al., 2007) which makes it a particularly attractive technique for early-warning purposes.

Nowadays, due to the development of computing technologies, the application of data-driven modelling approaches such as Machine Learning (ML) tools provides new opportunities to improve water quality (Haggerty et al., 2023; Singha et al., 2021) and management practices (Ahmed et al., 2024). Recent advances in ML applications have significantly improved predictive capabilities for estimating the occurrence of contaminants such as arsenic (Podgorski and Berg, 2020), nitrate (Mahlknecht et al., 2023), and fluoride (Podgorski and Berg, 2022) in porous aquifers. However, these techniques remain poorly explored to predict the presence of faecal bacteria in karst groundwater and could pose a significant advance for real-time water quality assessment and improve drinking water management.

This research is the first to explore the applicability of supervised ML algorithms to forecast the sanitary risk level from easy-to-measure water quality parameters in karst drinking water sources within the framework of early warning systems. For this purpose, two springs draining a karst aquifer were selected to i) determine the most suitable contamination indicator parameters at each source; ii) analyse the performance of ML algorithms to predict the sanitary risk levels; and iii) examine their potential use as an inexpensive groundwater protection tool.

2. Materials and methods

2.1. Test site

Ubrique town is located in a rural mountainous area (317 to 1395 m a.s.l.) in the NE part of Cádiz province (S Spain), approximately 80 km NE from the homonymous capital (Fig. 1A). It has a population of 16,439 inhabitants (INE, 2024), which fully depend on karst groundwater for human consumption. This area is characterized by a mean annual precipitation of 1305 mm (period 1984/85 to 2017/18, Martín-Rodríguez et al., 2023), mainly distributed as intense rain events during the wet period from autumn to spring.

Approximately 80–90 % of the drinking water consumed in this urban settlement is captured from Sierra de Ubrique binary karst aquifer (Fig. 1B, C), developed on a thick (> 500 m) sequence of Jurassic dolostones (lower formation) and limestones (upper formation) (Martín-Algarra, 1987). The geological structure is composed of NE-SW open anticline folds and synclines in which cores Cretaceous-Paleogene marls and marly-limestones can be found. Tertiary clay and sandstone formations (flysch-type formations) overthrust all the Mesozoic rock sequence.

Recharge in Sierra de Ubrique aquifer occurs (1) by diffuse infiltration of rainfall through 26 km^2 carbonate outcrops (autogenic component), and (2) by direct infiltration of surface flows in dolines (autogenic component) or from the flysch catchment (Albarrán stream; allogenic component; Fig. 1C). Hence, the term "binary" refers to the origin of recharge from carbonate or non-carbonate exposures (Marsaud, 1997). Natural drainage of Sierra de Ubrique aquifer is mainly produced through Cornicabra (349 m a.s.l.; Fig. 1D) and Algarrobal (317 m a.s.l.) perennial outlets (Martín-Rodríguez et al., 2023), which are captured to fulfil the drinking water demand of Ubrique town. In addition, an overflow spring (Garciago, 422 m a.s.l.) related to Algarrobal also drains groundwater from this system during high-water conditions.

Groundwater pressures in this area are related to rural activities such as goat and sheep livestock farming and the associated cheese industry. Furthermore, the presence of the wastewater treatment plant (WWTP) of Villaluenga del Rosario village, only 150 m upstream to the homonymous swallow hole (Fig. 1C), constitutes the main faecal contamination source (Fernández-Ortega et al., 2024a). Karst connections between Villaluenga swallow hole and Cornicabra, Algarrobal and Garciago springs were proved by means of two field tracer experiments (Martín-Rodríguez et al., 2023). The intense rain episodes produce diffuse recharge into the aquifer but also activate the allochthonous component through swallow holes, which introduces a great amount of suspended sediment associated with bacterial activity (Fernández-Ortega et al., 2024a). In contrast, the mobilization of para-autochthonous sediment from inner conduits has been demonstrated to be free of living faecal bacteria.

2.2. Monitoring network and microbiological analysis

The monitoring network was deployed between hydrological years 2020/21 to 2022/23 and comprises the permanent karst springs, where continuous measurements (15 min measuring rate) of water level (Odyssey®; Dataflow Systems Limited, Christchurch, New Zealand) in addition to electrical conductivity, turbidity and Tryptophan-Like-Fluorescence (TLF) (GGUN FL30®; Albilia Sarl, Switzerland) were recorded. The field fluorometer TLF optical sensor (λ_{ex} = 280 nm, λ_{em} =

360 nm) was calibrated with a L-tryptophan laboratory standard of analytical grade (CAS: 73–22–3; Sigma-Aldrich, Merck KGaA, Darmstadt, Germany). Likewise, the turbidity channel (λ_{ex} = 660 nm, λ_{em} = 860 nm) was calibrated using a 1000 NTU formazin standard (Sigma-Aldrich).

A total of 194 groundwater samples were collected from Cornicabra (n = 106) and Algarrobal (n = 88) capture points. 100 mL sterile plastic vials were filled with a groundwater aliquot and refrigerated at 12 °C in the dark and taken to the laboratory for the analysis no later than 12 h after collection. *E. coli* was then determined as the most probable number (MPN) per 100 mL following the Colisure® Quanti-Tray/2000 method (IDEXX Laboratories Inc., Westbrook, USA), which is approved by the U.S. Environmental Protection Agency and included in the Standard Methods for Examination of Water and Wastewater (APHA, AWWA, WEF, 2023). The microbial detection range of the colorimetric/fluorescence-based technique is from 1–2419 MPN/100 mL and method failure rate was determined to be 20 % by Olstadt et al. (2007). When *E. coli* counts exceeding the upper detection limit were expected, the samples were diluted with ultrapure water.

2.3. Statistical analysis

2.3.1. Sanitary risk assessment and selection of predictor variables

The sanitary risk assessment was carried out following the guidelines published by the WHO (1997), according to microbiological activity in drinking water sources. Hence, a classification based on increasing orders of magnitude of *E. coli* counts per 100 mL is defined by five classes: <1 (none), 1 to <10 (low), 10 to <100 (medium), 100 to <1000 (high) and >1000 counts (very high).

The use of proxy (surrogate) parameters can provide indirect information about the presence of a specific contaminant, coming through tedious analytical methods or expensive technologies. To select the optimal contamination indicator parameter for the modelling tasks, an analysis of variance (ANOVA; Bingham and Fry, 2010) between continuous groundwater parameters (Q, EC, turbidity, TLF) and sanitary risk levels was conducted. In each test the null hypothesis was that all group means are equal. The analysis includes the available predictors and those with *p-value* < 0.05 (Fisher, 1925) are considered for the ML models.

2.3.2. Machine learning classifiers

Within the frame of supervised learning techniques, the dataset is structured in "labelled" output (or target) variables (e.g. sanitary risk classes) (Rashidi et al., 2023). Individual algorithms are then trained with the aim of predicting the output using the remaining variables within the dataset (e.g. turbidity, TLF, etc.) and recognize patterns between them.

The selection of the most suitable modelling tools for a particular application is challenging. In this study, ten commonly applied ML approaches are compared (Fig. 2): *K-Nearest Neighbors* (KNN; Cover and Hart, 1967); *Radial Basis Function-Support Vector Machines* (RBF-SVM; Moguerza and Muñoz, 2006); *Gaussian Process* (Rasmussen and Williams, 2006); *Decision Tree* (DT; Quinlan, 1986); *Random Forest Decision Tree* (RF; Breiman, 2001); *Neural Network* (NNet; McCulloch and Pitts, 1943); *Ada Boost* (AB; Freund and Schapire, 1997); *Naive Bayes* (NV; Duda and Hart, 1973); *Quadratic Discriminant Analysis* (QDA; McLachlan, 1992); *Logistic Regression* (LR; Cox, 1958).

While each of these methods could potentially be used with a variety of settings and procedures for model selection, model configurations typical for most of their applications were considered for the modelling tasks. The scikit-learn v1.5.1 library function is incorporated in Python v3.11.5 for the implementation of ML algorithms.

2.3.3. Model training and performance assessment

The quick variations of water quality in karst groundwater as a response to aquifer recharge processes determine the sampling periodicity (Stevanovic and Stevanovic, 2021). A monthly or weekly sampling strategy during low-flow intervals might be increased to daily or hourly during flood events to accurately record significant changes in water parameters. This might lead to class imbalance issues, where some classes are underrepresented compared to others, and severely impact the model performance, inducing biased predictions and inaccurate

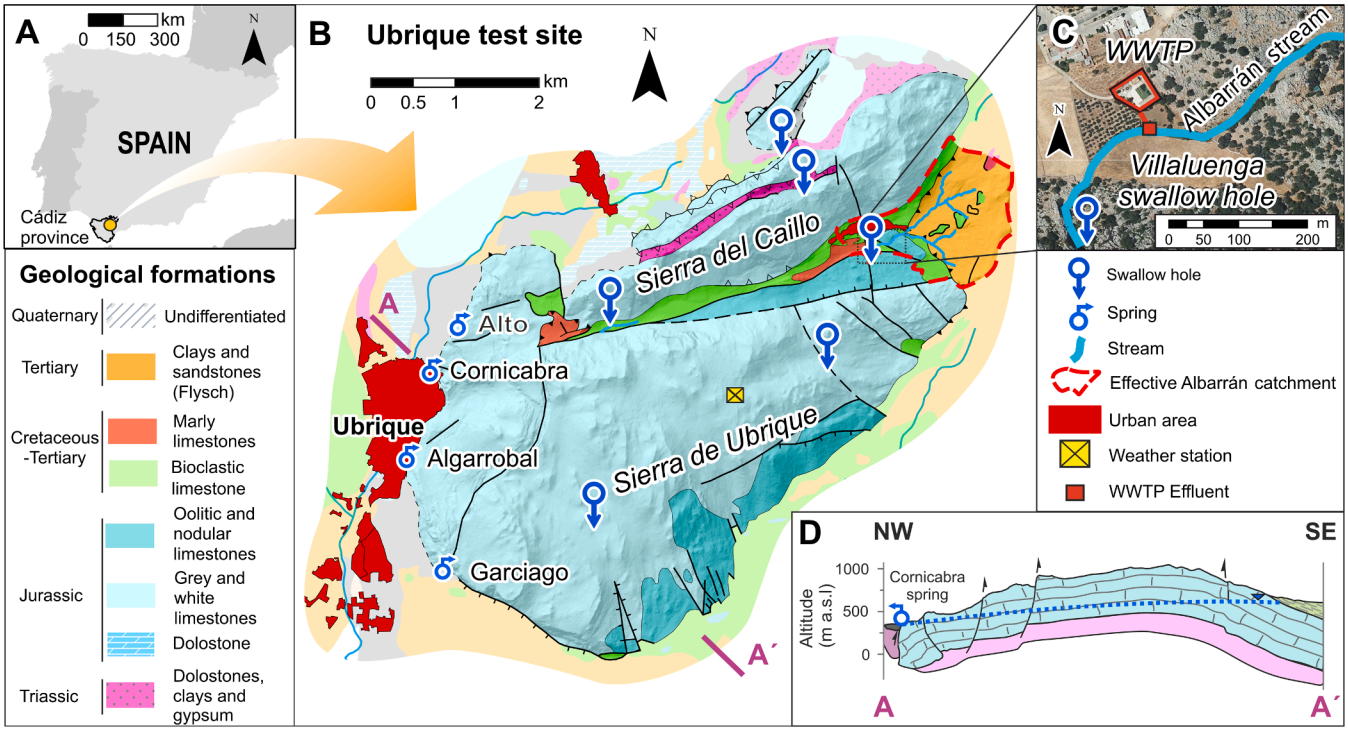

Fig. 1. A) Location of the study area, B) hydrogeological setting, C) zoomed out area of the allogenic infiltration site, and D) interpretative hydrogeological cross-section.

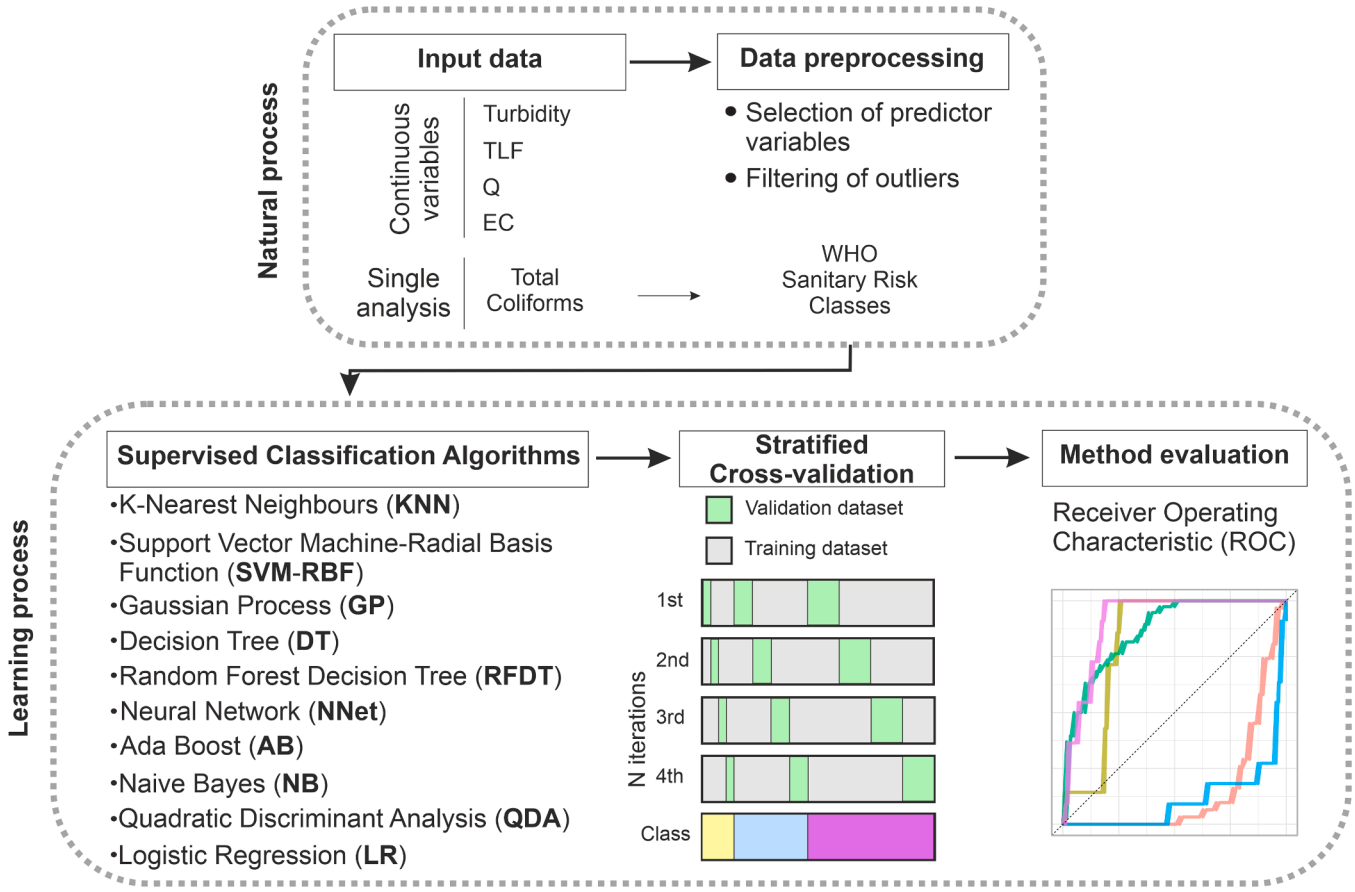

Fig. 2. Methodological sketch of the research, from field data collection to the application of supervised Machine Learning algorithms.

results. Stratified K-Fold Cross-Validation (Pedregosa et al., 2011) is an advanced form of cross-validation that is particularly useful when working with datasets that have an unbalanced distribution of classes. This technique ensures that each fold of the dataset contains approximately the same percentage of samples of each class as the complete set, making the training and validation process (Fig. 2) fair and more reliable.

The simplest approach to select an optimal model for prediction is to compare the error rates estimated from cross-validation, where the modelling method with the lowest error estimate is determined as the best one to use. Common approaches are derived from success rate curves, prediction rate curves (Chung and Fabbri, 2003) or receiver operating characteristic (ROC) curves (Beguería, 2006; Brenning, 2005; Frattini et al., 2010; Gorsevski et al., 2006; Hanley and McNeil, 1983). The effectiveness of a classifier can be assessed in terms of the last-mentioned method, which constitutes a plot of the proportion of true positive results against the proportion of false positive results. The area under this curve (AUC) is a measure of the effectiveness of the classifier. It will be 1 for a perfect classifier and 0.5 if the classifier is performing no better than a random choice.

3. Results

3.1. Hydrogeological behaviour of the drinking water sources

Spring discharge shows a variation of two orders of magnitude between the minimum and maximum values at both springs during the study period (Table 1). Mean and maximum values of EC and, specially, turbidity and TLF, are roughly greater in Algarrobal compared to Cornicabra. In the same way, the highest mean *E. coli* value was registered at Algarrobal, almost double that of Cornicabra spring. In addition, these Faecal Indicator Bacteria (FIB) data show a greater variability in

Table 1
Statistical parameters of groundwater parameters (spring discharge, electrical conductivity, turbidity, and TLF) and Faecal Indicator Bacteria (FIB) as *E. coli* measured in water samples collected at karst springs of the study area. Legend: (n) - number of samples, (Min) - minimum value, (Max) - maximum value, (Mean) - arithmetic average value and (SD) - standard deviation.

		Spring discharge (L/s)	Electrical conductivity (μS/cm)	Turbidity (NTU)	TLF (eq. ppb)	*E. coli* (MPN/100 mL)
Cornicabra (n = 105)	Max	1868	298	31	71	2419*
	Mean	456	271	6	14	129
	Min	1	227	0	3	1
	SD	505	13	7	10	302
Algarrobal (n = 88)	Max	1767	514	258	120	4839**
	Mean	424	326	26	20	301
	Min	15	256	0	5	1
	SD	460	46	48	25	724

* Method Quantification Limit,.
** Method Quantification Limit after Dilution Factor 2.

Algarrobal spring (SD = 724 MPN / 100 mL).

The two investigated springs present distinctive responses to rain events, despite draining the same aquifer. On the one hand, Cornicabra spring (Fig. 3A) shows a quick spring discharge increase immediately after the rain input, followed by a smooth EC decrease. The highest bacterial activity was recorded at the beginning of the flood event, coinciding with the first turbidity peak, and the lowest values were observed during the highest spring discharge and TLF values. On the other hand, Algarrobal spring (Fig. 3B) shows a delayed response characterised by an increase of EC with TLF and turbidity. It highlights that the lowest bacterial activity was detected concomitant to the first turbidity and EC peak and posteriorly increases with the highest discharge rates.

3.2. Statistical significance of groundwater parameters

The relationship between *E. coli* activity and groundwater parameters is represented in Fig. 4 from biplots. Cornicabra spring data display lower dispersion between sanitary risk levels and TLF, logTLF, logTurbidity and EC, which is the only parameter to show an inversely proportional relationship. At this spring, only one sample was classified as "very high" risk, and hence, will not be considered for the ML analysis.

In the case of Algarrobal spring, all parameter data scatter widely but mantain a proportional statistical relationship. The presence of para-autochthonous sediment in Algarrobal spring samples is evidenced by high turbidity (> 50 NTU) values classified as "low" or "none" risk (Fig. 4). These samples will not be considered for the ML analysis due to the poor representativity for the corresponding sanitary risk class.

Given that sanitary risk assessment is determined by different levels based on the increasing magnitude of *E. coli* activity, the statistical analysis considers nominal categories. Thus, the data distribution of spring discharge, electrical conductivity, turbidity and TLF values within each sanitary risk category is represented in Fig. 5. The results of the ANOVA tests suggest that spring discharge, turbidity and TLF present well differentiated mean values within each sanitary risk level, and hence, these are statistically significant.

Cornicabra spring displays directly proportional median values of spring discharge (Fig. 5A), turbidity (Fig. 5C) and TLF (Fig. 5D) with increasing sanitary risk levels, while the opposite statistical relationship is observed with EC data (Fig. 5B). Furthermore, only one sample collected is classified as "very high" sanitary risk. Algarrobal spring shows proportional median values of all continuous parameters with increasing sanitary risk levels. Groundwater from this spring displays very low minimum TLF values at all risk levels (Fig. 5D). In Algarrobal spring, high turbidity values with some outlier samples exceed the threshold (4 NTU) established in the recently revised Spanish regulation for potable water (RD 3/2023) corresponding to "none" and "low" risk levels (Fig. 4C).

3.3. Machine learning classifier assessment

3.3.1. Single vs multiple classifiers

Before computing the definitive ML models, all of them were run to obtain their optimal configurations and to select the most favourable predictor of sanitary risk levels at both karst springs. This step provided a total of 190 different modelling results for each spring derived from the computation of the 10 tested classifiers with the 6 predictor parameters and the 13 possible combinations among them (A.1).

Single-predictor approaches show poor results for electrical conductivity (mean AUC of 0.64 in Cornicabra and 0.61 in Algarrobal; Table 2). The use of spring discharge as a predictor variable has a better performance in Algarrobal (0.75) in comparison to Cornicabra (0.66). The choice of TLF (and logTLF) as bacterial activity indicator is more successful in Cornicabra spring (mean AUC = 0.71 and 0.72, respectively) than in Algarrobal spring (Table 2). The highest AUC values were determined for turbidity (and its logarithmic transform) in both Cornicabra (0.73 and 0.73, respectively) and Algarrobal (0.75 and 0.77) springs.

In general, the modelling results by using single predictors yield slightly lower mean AUC values than those obtained with dual predictors (Table 2). The couples of spring discharge and turbidity (and logTurb) as well as logTurb+logTLF in Cornicabra spring or *Q*+logTurb in Algarrobal seem the most suitable combinations.

3.3.2. General model performance

After computing all ML models with dual predictors, the four most successful approaches (Gaussian Processes (GP), Neural Networks (NNet), Naïve Bayes (NB) and Quadratic Discriminant Analysis (QDA)) were selected for a more detailed assessment (Fig. 6). Specific dual predictor combinations such as TLF and turbidity in Cornicabra spring as well as turbidity and spring discharge or logTurb and EC in both Cornicabra and Algarrobal springs result in acceptable (> 0.75) AUC values. However, in general terms, the combination of logTurb with i) spring discharge and ii) logTLF provide the best fit (AUC > 0.80) in both permanent springs (Fig. 6).

In Cornicabra spring, *Q*+Turb approach in NNet, NB and QDA displays "high risk" with turbidity values > 10 NTU at relatively low flow (< 750 L/s) but with > 20 NTU for highest spring discharge rates (> 1500 L/s; Fig. 6). In contrast, the GP model only displays "medium risk" over 1250 L/s. The increase in risk class in Cornicabra spring is roughly

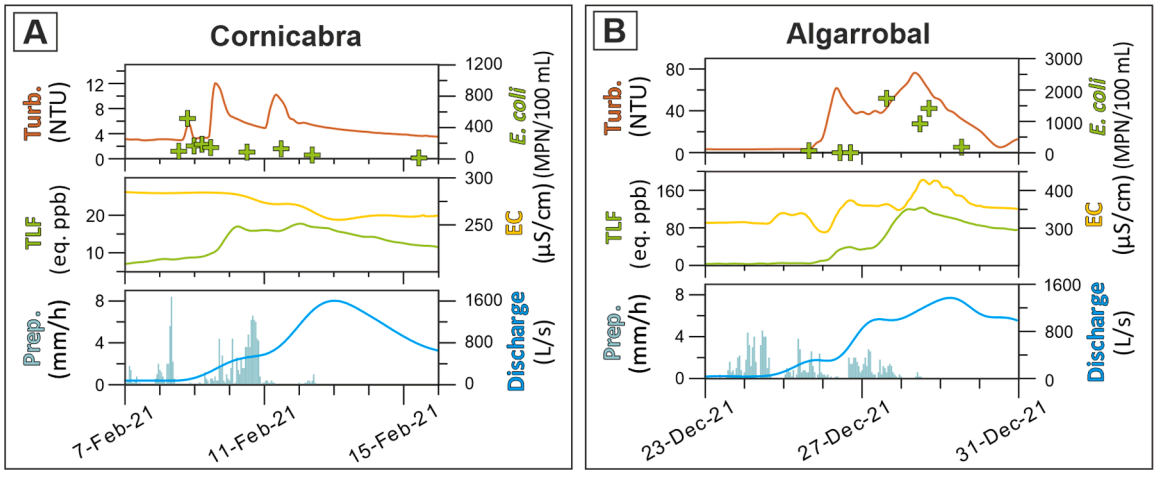

Fig. 3. Selected unitary flood events recorded at A) Cornicabra and B) Algarrobal springs showing hourly data from precipitation (Prep.), spring discharge, electrical conductivity (EC), turbidity (Turb.) and TLF with *E. coli* analysis.

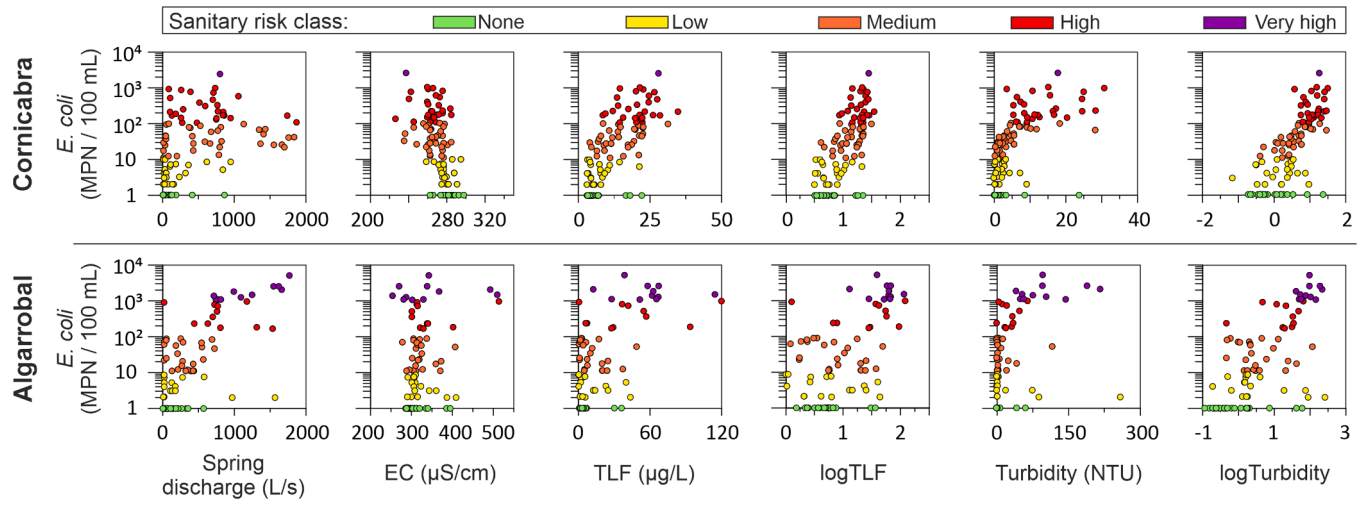

Fig. 4. Biplot between *E. coli* and continuous parameters (spring discharge, electrical conductivity (EC), TLF, logTLF, turbidity, and logTurbidity) measured in Cornicabra and Algarrobal spring waters.

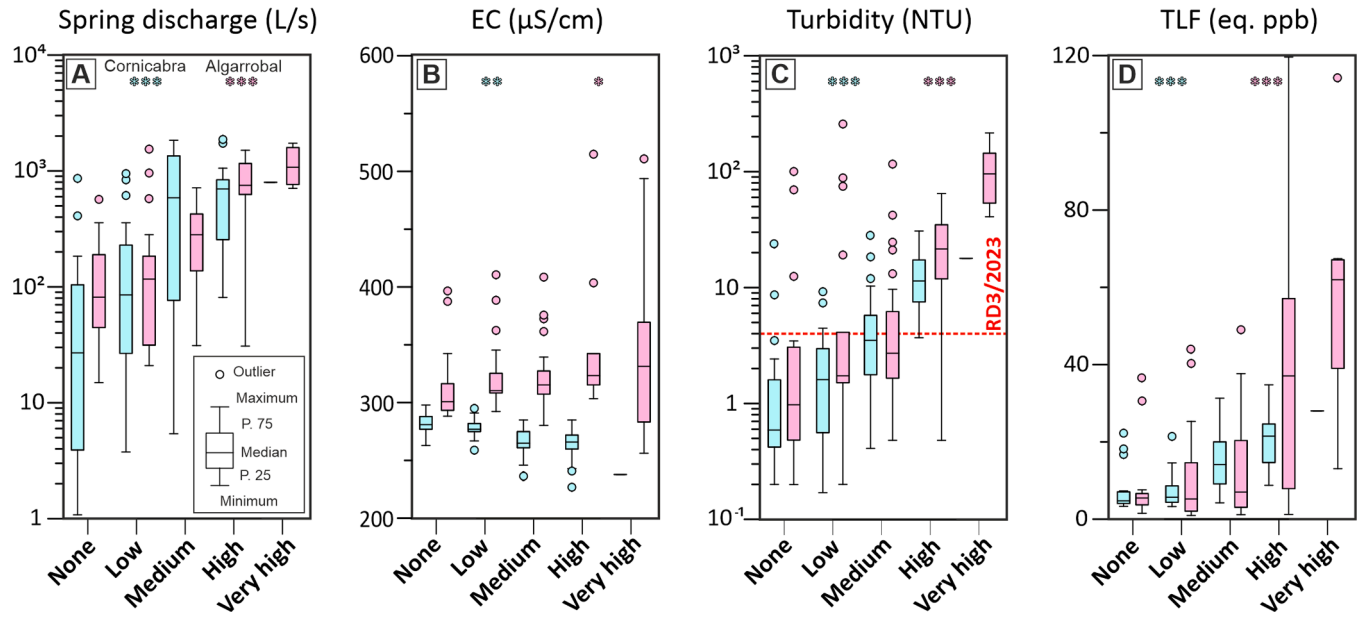

Fig. 5. Box plot diagrams representing the statistics of proxy parameter data measured at Cornicabra (blue) and Algarrobal (pink) karst springs: A) spring discharge, B) electrical conductivity, C) turbidity and D) TLF associated with each sanitary risk level estimated at drinking water sources. P-values are denoted as * <0.05, ** <0.01, and *** <0.001. Red line indicates the legal threshold for turbidity in the Spanish regulation (RD 3/2023).

proportional to TLF and turbidity, which show "low risk" or "none" under 20 eq. ppb and 5 NTU, respectively (Fig. 5).

In Algarrobal spring, Q+Turb approach displays "medium risk" up to ≈ 800 L/s and 80 NTU in NB and QDA but up to approximately 160–200 NTU in GP and NNet (Fig. 6). "High risk" is usually associated with flow > 800 L/s but turbidity below 60 NTU. Finally, "very high risk" is found during typical flood event conditions with spring discharge rates and turbidity levels exceeding the aforementioned thresholds. A common TLF threshold around 40 eq. ppb allows to define the limit between "medium" and "high risk" classes. Generally, "none" risk level is restricted to minimum values (i.e. background levels) of the considered water parameters.

3.3.3. *Single class classifier*

The two most successful dual-parameter approaches (logTurb+*Q* and logTurb+logTLF) for sanitary risk prediction display some differences while classifying individual risk levels. Receiver Operator Characteristic (ROC) curves (Fig. 7) are computed to compare the obtained results at both karst springs. On the one hand, the logTurb and Q curves display some overlapping between Cornicabra and Algarrobal, which is especially noticeable at "none", "low" and "medium" risk levels (Fig. 7A). On the other hand, logTurbidity and logTLF combination only shows a minor ROC overlap between the two springs at "medium" risk level (Fig. 7B). A better result is found in Algarrobal spring for "none" class while both approaches provide a notably worse result matching "high" sanitary risk category.

The best classified risk level is "very high" (mean AUC = 0.97) in Algarrobal spring, followed by "none" (mean AUC = 0.94) at the same outlet (Table 3). Likewise, in Cornicabra spring, "high" category presents a mean AUC of 0.91 while at "none" is 0.82. The worst classified risk level is "medium" at both outlets (mean AUC of 0.73 and 0.71, in Cornicabra and Algarrobal, respectively). As a general trend, some sanitary risk classes in Cornicabra ("low" and "medium") and in Algarrobal ("low", "medium" and "high") display lower AUC values

Table 2
Mean area under the curve (AUC) values for single (spring discharge (Q); electrical conductivity (EC); turbidity (Turb); and Tryptophan-Like-Fluorescence (TLF)) and multiple predictors combination obtained from the 10 computed ML classifiers for both permanent karst springs.

	Single predictor					Dual predictors										Multiple predictors	
	Q	EC	Turb	logTurb	TLF	logTLF	Q+EC	Q+Turb	Q+logTurb	Q+TLF	Q+logTLF	EC+Turb	EC+logTurb	EC+TLF	EC+logTLF	Turb+TLF	Turb+logTLF	TLF+logTurb	logTurb+logTLF
Cornicabra	0.66	0.64	0.73	0.73	0.71	0.72	0.66	0.76	0.76	0.72	0.72	0.72	0.73	0.70	0.70	0.75	0.75	0.75	0.76
Algarrobal	0.75	0.61	0.75	0.77	0.66	0.66	0.73	0.77	0.80	0.74	0.74	0.71	0.75	0.69	0.67	0.72	0.72	0.76	0.76

compared to extreme classes (Table 3). For GP and NNet for "very high" risk levels, AUC values for logTurb+*Q* and logTurb+logTLF are equal, but shows systematic worse classification rate success in “none” risk (Table 3). Nevertheless, the combination of logTurb+*Q* generally provides a better prediction result regardless of the applied ML model. In contrast, the results from Cornicabra spring display a strong dependence on the selected ML model. Hence, NNet has almost identical results with both predictor combinations while GP and QDA showed higher AUC values for the logTurb+*Q* approach at every category except for “low” risk. NB is the only ML classifier to deliver higher AUC values for every class except “high” risk using logTurb+logTLF in Cornicabra spring.

4. Discussion

4.1. Selection of spring-specific proxy parameters

Spring discharge is a commonly controlled parameter given that hydrodynamic variations determine many of the chemical changes in groundwater (Goldscheider and Drew, 2007) and its early-warning implications have been previously explored (Auckenthaler et al., 2002). In this research, spring discharge in Algarrobal spring shows a notably higher mean AUC value compared to Cornicabra (Table 2) due to the direct relationship observed between such parameter and the activity of *E. coli* (Fig. 4) or the WHO sanitary risk levels (Fig. 5A) in the first spring. Therefore, the transfer of faecal bacteria through this subsystem is more dependent on hydrodynamic conditions, probably due to the preferential connection to concentrated recharge points, such as the Villaluenga swallow hole (Martín-Rodríguez et al., 2023).

EC is a commonly used indicator of water quality (Thompson et al., 2012) and, when coupled to spring discharge, is used to explain recharge processes (Liñán-Baena et al., 2009). The inverse correlation of EC with WHO sanitary risk levels in Cornicabra spring (Fig. 5B) is related to the arrival of recently infiltrated rainwater (with high bacterial load), which causes increase of spring discharge and the concurrent dilution (Fig. 3A). The notable piston-flow from the saturated zone observed in Algarrobal spring at the beginning of a flood event (Fig. 3B) is responsible for the high EC values registered with low bacterial activity (Fig. 5B), resulting in low AUC values (Table 2).

The use of turbidity as a contamination indicator has been widely explored given that pathogens can adsorb onto particles (Dhand et al., 2009). In the present study, this fact is also reflected as high AUC values for turbidity as a single predictor (Table 2). However, the occurrence of high turbidity values in absence of faecal contamination (Fig. 3B) is a commonly observed process in karst system due to the mobilization of (para-autochthonous) sediment from the saturated zone due to piston flow mechanisms (Mahler and Lynch, 1999; Pronk et al., 2007). This was also observed during the initial response of Ubrique test site springs, but especially noticeable in Algarrobal (Fernández-Ortega et al., 2024a) and evidenced as outlier values within the “none” and “low” sanitary risk levels in Fig. 5C. Thus, the simultaneous detection of turbidity caused by mobilization of sediment from within conduits (presumably without viable *E. coli*) and that associated with recently infiltrated runoff (with bacterial activity) may explain the ambiguities concerning the correlation of this parameter with sanitary risk levels at the investigated sources.

L-Tryptophan molecule has been described as a product of bacterial activity (Arana et al., 2004; Cammack et al., 2004; Hudson et al., 2007) and its fluorescence properties constitute an effective tracer able to quickly infer microbial contamination (Baker et al., 2015; Nowicki et al., 2019). Hence, this fact makes this parameter especially suitable for swallow aquifer systems in urbanized areas affected by septic leakages, like the ones described by Sorensen et al. (2015) and Dapkus et al. (2023). Its application to karst systems as an early-warning parameter was recently tested in an alpine aquifer with little success, given that the low peak T fluorescence values (related to protein-like compounds) are not suitable to determine precise bacterial values (Frank et al., 2018). In

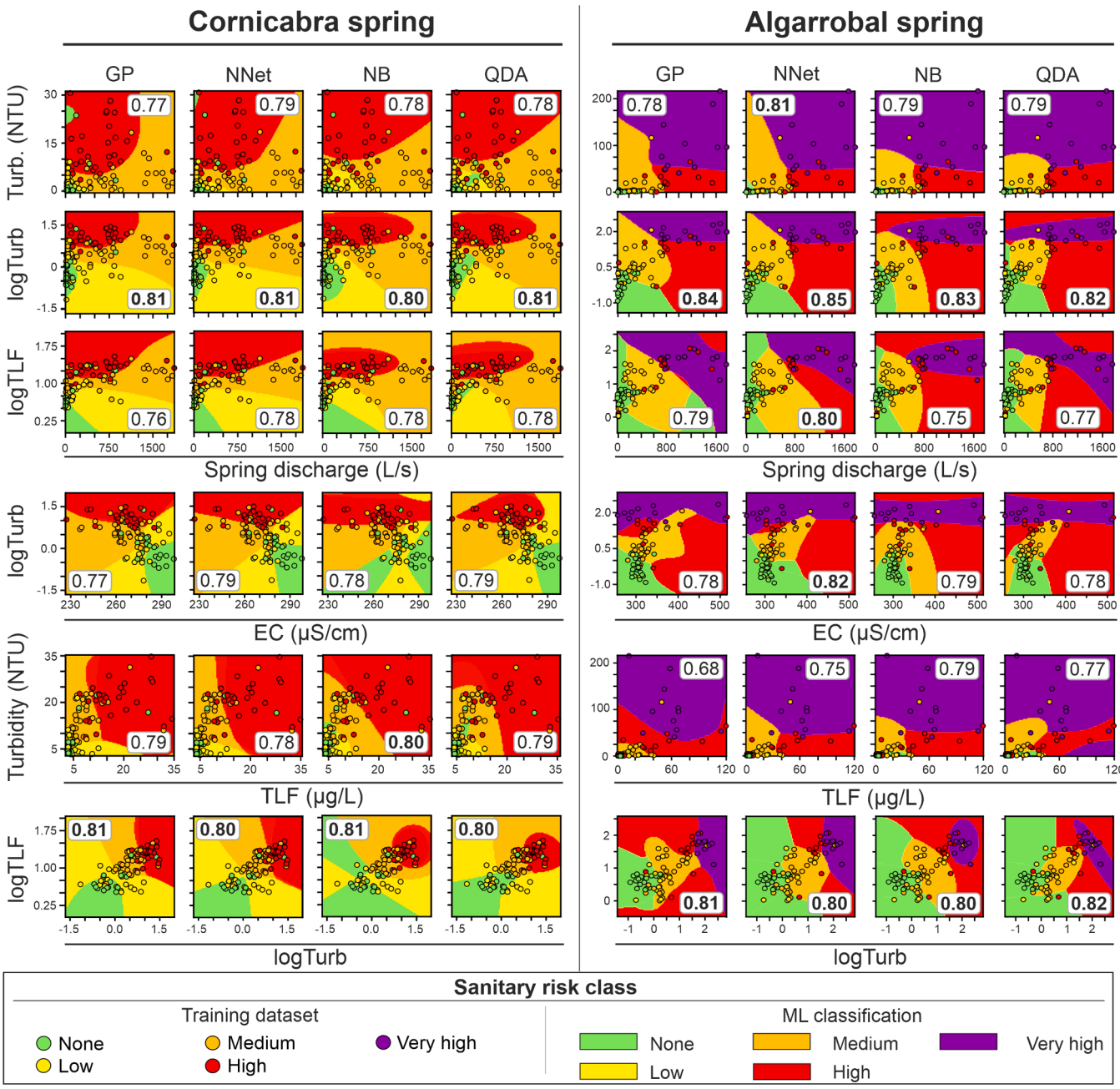

Fig. 6. Best Machine Learning classifiers (Gaussian Process, GP; Neural Network, NNet; Naive Bayes, NB; and Quadratic Discriminant Analysis, QDA) for sanitary risk levels at Cornicabra and Algarrobal springs. The goodness of performance is measured through Area Under the Curve (AUC) value, included in the white labels with values in bold (AUC $\geq$ 0.8).

binary karst aquifers, such as Sierra de Ubrique, the detection of organic compounds which have been mobilized with suspended sediments via allogenic recharge, might be hindered due to the interferences caused by turbidity in measuring devices. This provoked the relatively low mean AUC values in Algarrobal spring for TLF as a single predictor (Table 2) could be due to the great magnitude of turbidity variations (Table 1). These findings differ from the results presented by Sorensen et al. (2015), who reported an AUC of 0.92 using only TLF as a predictor. The use of TLF cannot substitute for conventional bacterial determination methods but its combination with complementary parameters might improve its application as proxy parameter for organic contamination assessment.

The aquifer geometry and the development of the conduit system determine the hydrodynamic processes controlling spring discharge variations and associated contaminant transport in karst aquifers. As an example, the two permanent springs draining Sierra de Ubrique system show distinctive hydrogeological and contamination dynamics (Fig. 3) despite sharing, to a certain extent, the recharge area (Martín-Rodríguez et al., 2023). Hence, the spring-specific assessment and the correct identification of contamination proxy (surrogate) parameters are essential for the application of the adequate early-warning strategies.

4.2. *Performance of supervised ML in water quality*

The use of ML techniques may overcome many of the limitations of traditional methods such as time-consuming cultures or expensive chemical reagents for real-time monitoring of water quality (Bedell et al., 2022; Pras and Mamane, 2023). Nevertheless, the selection of the

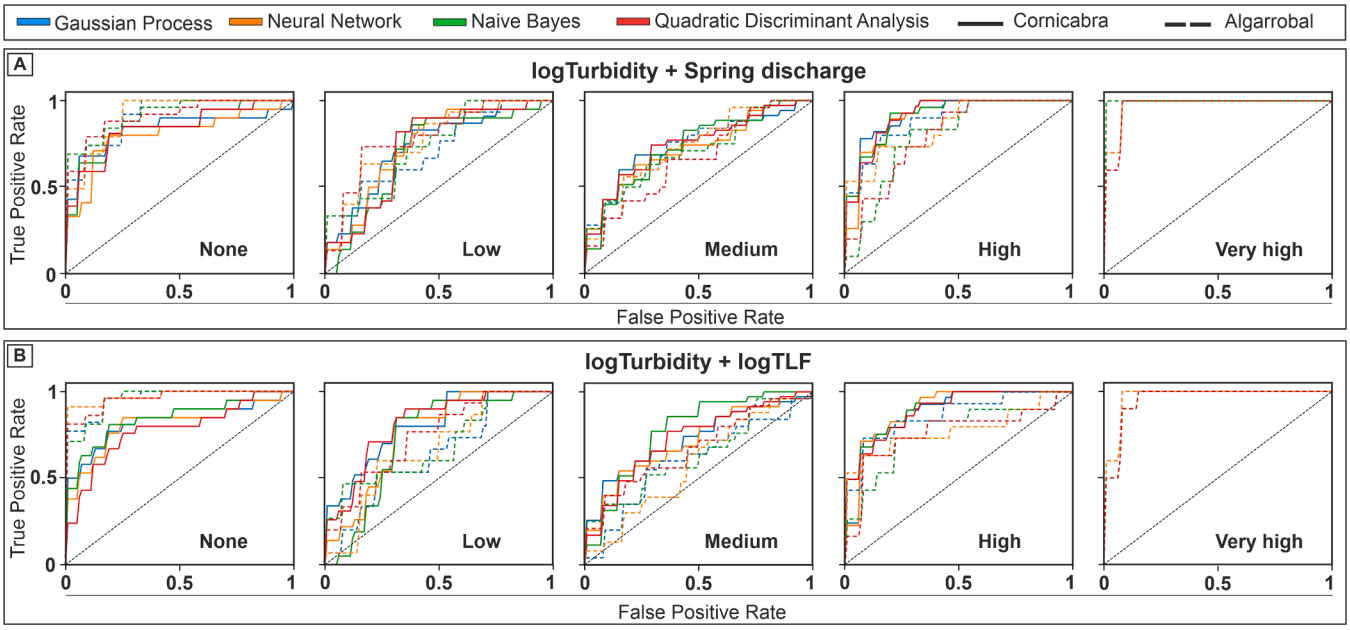

Fig. 7. Receiver operator characteristic (ROC) curves for Gaussian Process, Neural Network, Naive Bayes and Quadratic Discriminant Analysis classifiers of each sanitary risk level in Cornicabra (straight line) and Algarrobal springs (dashed line).

Table 3
Area under the curve (AUC) values corresponding to individual sanitary risk classes for logTurb combination with spring discharge (Q) and logTLF obtained from Gaussian Process (GP), Neural Network (NNet), Naïve Bayes (NB) and Quadratic Discriminant analysis (QDA) at permanent karst springs of Sierra de Ubrique aquifer.

		Cornicabra spring		Algarrobal spring	
	Class	logTurb+*Q*	logTurb +logTLF	logTurb+*Q*	logTurb +logTLF
GP	None	0.84	0.82	0.91	0.96
	Low	0.74	0.81	0.71	0.64
	Medium	0.74	0.72	0.74	0.6
	High	0.92	0.88	0.89	0.86
	Very high	–	–	0.97	0.97
NNet	None	0.8	0.81	0.91	0.97
	Low	0.75	0.76	0.77	0.66
	Medium	0.72	0.71	0.73	0.58
	High	0.9	0.89	0.85	0.78
	Very high	–	–	0.97	0.97
NB	None	0.84	0.85	0.92	0.95
	Low	0.7	0.73	0.74	0.69
	Medium	0.73	0.77	0.71	0.63
	High	0.91	0.9	0.79	0.76
	Very high	–	–	0.99	0.95
QDA	None	0.84	0.78	0.91	0.96
	Low	0.73	0.81	0.79	0.74
	Medium	0.74	0.73	0.66	0.67
	High	0.91	0.89	0.8	0.76
	Very high	–	–	0.97	0.95

appropriate Machine Learning approach for solving a specific problem supposes a challenging issue that might be conditioned on data features such as statistical dependence among variables, clustering and the targeted accuracy (Huerta et al., 2022). Traditional linear regression (LR) models are commonly used due to their simplicity, efficiency, and applicability (Singha et al., 2021). As an example, Sorensen et al. (2015) successfully applied this approach to discriminate between sanitary risk classes using TLF as a predictor. The application of linear approaches might fit for Cornicabra spring data, which show an apparent linear relationship between *E. coli* and EC, turbidity and TLF (Fig. 4), but is inefficient for Algarrobal spring data, which exhibit a greater dispersion. Therefore, classification models were considered for this research instead of regression approaches.

Among the tested ML algorithms, the worst results were provided by SVM-RBF, DT and AB (A.1). These models could be limited by noisy (high dispersion) data (Nettleton et al., 2010) and might require larger datasets (Althnian et al., 2021). Conversely, GP, NNet, NB and QDA, which showed the best results for both datasets (Fig. 6), usually capture complex nonlinear patterns (like some karst spring responses; Fernández-Ortega et al., 2024a) better than DT or AB (Mohammadagha, 2025). These models also provide smoother and continuous decision boundaries between classes instead of the rectangle limits provided by DT, RF or AB (A.2). This highlights that depending on the hydrogeological behaviour, the related contaminant sources, their nature, load and transport mechanisms within the aquifer, the selection of the optimal statistical approach for water quality assessment might vary.

4.3. Transferability and integration into early warning systems for real-time sanitary risk assessment

The outcomes of this research can be transferred to the management of any type of drinking water system, regardless of the size of the population supplied, the type of aquifer, the degree of anthropisation, or the nature of the contaminants. This can be easily achieved by adapting the monitored parameters (Fig. 2) to overcome system-specific issues and selecting the optimal ML model that best fits the registered data. As an example, Bedell et al. (2022) successfully developed a similar approach through ML classification models to assess water quality using TLF in a river used for drinking water supply.

The future development of early-warning tools should be focused on in situ real-time monitoring (Sorensen et al., 2015), data transmission, on-line processing and warning dissemination (Fernández-Ortega et al., 2024b) to water authorities to provide a reliable assessment of water quality in drinking water sources. Hence, the development of ML tools for inferring the presence of difficult-to-measure water parameters (such as bacterial activity) constitutes a promising research line for scientific-technical advances. Within this context, the use of soft-sensors,

which utilise data-driven models to predict contaminant concentrations from a set of input variables (e.g., nitrate; Stamenković et al., 2020), provides a flexible and adaptable framework for monitoring contaminant concentrations in different environmental settings (Chaves et al., 2025).

5. Conclusions

This is the first study to investigate the use of supervised ML methods in karst groundwater for the indirect sanitary risk assessment of drinking water sources. The developed methodological framework provides significant milestones in the field of EWS for karst systems, producing real-time insights to support decision makers.

The different karst dynamics of individual sources require that the monitored water parameters are adapted to site-specific features, even though these drain the same recharge area in the case of the investigated site. The combination of two or more proxy parameters that are indicative of hydrodynamic and hydrochemical processes within the aquifer seems the best option to develop more robust predictive models.

Due to the heterogeneity of karst systems, the hydrogeological responses to rain events rarely correspond to strictly linear processes. Hence, Bayesian probabilistic models such as Gaussian Processes, Naïve Bayes and Quadratic Discriminant analysis have proven to be extremely useful to reproduce the complex behaviour of these aquifers. Furthermore, Neural Networks can capture nonlinear patterns even with a limited database, what makes this model especially useful in case studies with limited datasets.

The obtained ML models are coherent with the results derived from tracer tests and may be considered as a prediction tool to quickly determine sanitary risk in the drinking water sources. However, they require a proper validation by occasional water sampling and traditional culture methods according to site-specific features, which also provide a feedback to the ML model. These advances would contribute to the improvement of source protection strategies from the implementation of early warning tools for water contamination in a changing and threatened world.

CRediT authorship contribution statement

Jaime Fernández-Ortega: Writing – review & editing, Writing – original draft, Visualization, Methodology, Investigation, Data curation, Conceptualization. **Juan Antonio Barberá:** Writing – review & editing, Supervision, Project administration, Investigation, Funding acquisition, Conceptualization. **Bartolomé Andreo:** Writing – review & editing, Supervision, Project administration, Funding acquisition, Conceptualization.

Declaration of competing interest

The authors declare that they have no competing financial or personal interests that could have influenced the work presented in this paper.

Acknowledgements

This research is a contribution to the PRIMA funded European project KARMA (Karst Aquifer Resources availability and quality in the Mediterranean Area – ANR-18-PRIM-0005), the Spanish project, PCI2019–103675 of the International Combined Programme of the Ministry of Science, Innovation and Universities, the project PID2019–111759RB-I00 as well as by the Research Group RNM-308 of the Junta de Andalucía, funded by the Autonomous Government of Andalusia (Spain). The authors thank the local government of Ubrique and the water company "Empresa Mixta de Aguas de Ubrique" for their collaboration.

Funding for open access charge: Universidad de Málaga / CBUA.

Supplementary materials

Supplementary material associated with this article can be found, in the online version, at doi:10.1016/j.watres.2025.125060.

Data availability

Data will be made available on request.

References

Ahmed, A.A., Sayed, S., Abdoulhalik, A., Moutari, S., Oyedele, L., 2024. Applications of machine learning to water resources management: a review of present status and future opportunities. J. Clean. Prod. 441, 140715. https://doi.org/10.1016/j.jclepro.2024.140715.

Althnian, A., AlSaeed, D., Al-Baity, H., Samha, A., Dris, A.B., Alzakari, N., Abou Elwafa, A., Kurdi, H., 2021. Impact of dataset size on classification performance: an empirical evaluation in the medical domain. Appl. Sci. 11 (2), 796. https://doi.org/10.3390/app11020796.

American Public Health Association, American Water Works Association, & Water Environment Federation, 2023. Standard Methods For the Examination of Water and Wastewater, 24th ed. APHA Press.

Arana, I., Seco, C., Epelde, K., Muela, A., Fernández-Astorga, A., Barcina, I., 2004. Relationships between Escherichia coli cells and the surrounding medium during survival processes. Antonie Leeuwenhoek 86 (2), 189–199. https://doi.org/10.1023/B:ANTO.0000036146.28808.93.

Ashbolt, N.J., 2004. Microbial contamination of drinking water and disease outcomes in developing regions. Toxicology 198 (1–3), 229–238. https://doi.org/10.1016/j.tox.2004.01.030.

Auckenthaler, A., Raso, G., Huggenberger, P., 2002. Particle transport in a karst aquifer: natural and artificial tracer experiments with bacteria, bacteriophages, and microspheres. Water. Sci. Technol. 46 (3), 131–138. https://doi.org/10.2166/wst.2002.0072.

Baker, A., Cumberland, S.A., Bradley, C., Buckley, C., Bridgeman, J., 2015. To what extent can portable fluorescence spectroscopy be used in the real-time assessment of microbial water quality? Sci. Total. Environ. 532, 14–19. https://doi.org/10.1016/j.scitotenv.2015.05.114.

Bedell, E., Harmon, O., Fankhauser, K., Shivers, Z., Thomas, E., 2022. A continuous, in-situ, near-time fluorescence sensor coupled with a machine learning model for detection of fecal contamination risk in drinking water: design, characterization and field validation. Water. Res. 220, 118644. https://doi.org/10.1016/j.watres.2022.118644.

Beaudeau, P., Le, T.A., Zeghnoun, A., Zanobetti, A., Schwartz, J., 2012. A time series study of drug sales and turbidity of tap water in Le Havre, France. J. Water. Health 10 (2), 221–235. https://doi.org/10.2166/wh.2012.157.

Beguería, S., 2006. Validation and evaluation of predictive models in hazard assessment and risk management. Nat. Hazards 37, 315–329. https://doi.org/10.1007/s11069-005-5182-6.

Bingham, N.H., Fry, J.M., 2010. The analysis of variance (ANOVA). Regression (Springer Undergraduate Mathematics Series). Springer. https://doi.org/10.1007/978-1-84882-969-5_4.

Breiman, L., 2001. Random forests. Mach. Learn. 45 (1), 5–32. https://doi.org/10.1023/A:1010933404324.

Brenning, A., 2005. Spatial prediction models for landslide hazards. Nat. Hazards Earth Syst. Sci. 5 (6), 853–862. https://doi.org/10.5194/nhess-5-853-2005.

Cammack, W.L., Kalff, J., Prairie, Y.T., Smith, E.M., 2004. Fluorescent dissolved organic matter in lakes: relationships with heterotrophic metabolism. Limnol. Ocean. 49 (6), 2034–2045. https://doi.org/10.4319/lo.2004.49.6.2034.

Chaves, A., Martín, C., Llopis Torres, L., Díaz, M., Fernández-Ortega, J., Barberá, J.A., Andreo, B., 2025. A soft sensor open-source methodology for inexpensive monitoring of water quality: a case study of NO_3^- concentrations. J. Comput. Sci. 85, 102522. https://doi.org/10.1016/j.jocs.2024.102522.

Chung, C.J.F., Fabbri, A.G., 2003. Validation of spatial prediction models for landslide hazard mapping. Nat. Hazards 30, 451–472. https://doi.org/10.1023/B:NHAZ.0000007172.62651.2b.

Cover, T., Hart, P., 1967. Nearest neighbor pattern classification. IEEe Trans. Inf. Theory. 13 (1), 21–27. https://doi.org/10.1109/TIT.1967.1053964.

Cox, D.R., 1958. The regression analysis of binary sequences. J. R. Stat. Soc. 20 (2), 215–242. https://doi.org/10.1111/j.2517-6161.1958.tb00292.x.

Dapkus, R.T., Fryar, A.E., Tobin, B.W., Byrne, D.M., Sarker, S.K., Bettel, L., Fox, J.F., 2023. Utilization of tryptophan-like fluorescence as a proxy for E. coli contamination in a mixed-land-use karst basin. Hydrology 10 (4), 74. https://doi.org/10.3390/hydrology10040074.

Delaire, C., Peletz, R., Kumpel, E., Kisiangani, J., Bain, R., Khush, R., 2017. How much will it cost to monitor microbial drinking water quality in sub-Saharan Africa? Env. Sci. Technol. 51 (11), 5869–5878. https://doi.org/10.1021/acs.est.6b06442.

Dhand, N.K., Toribio, J.A., Whittington, R.J., 2009. Adsorption of mycobacterium avium subsp. Paratuberculosis to soil particles. Appl. Env. Microbiol. 75 (17), 5581–5585. https://doi.org/10.1128/AEM.00378-09.

Duda, R.O., Hart, P.E., 1973. Pattern Classification and Scene Analysis. Wiley.

Fernández-Ortega, J., Barberá, J.A., Andreo, B., 2024a. Real-time karst groundwater monitoring and bacterial analysis as early warning strategies for drinking water

supply contamination. Sci. Total. Environ. 912, 169539. https://doi.org/10.1016/j.scitotenv.2023.169539.
Fernández-Ortega, J., Ulloa-Cedamanos, F., Barberá, J.A., Batiot-Guilhe, C., Jourde, H., Andreo, B., 2024b. A common framework for the development of spring water contamination early warning systems in western Mediterranean karst areas: spanish and French sites. Sci. Total. Environ. 956, 177294. https://doi.org/10.1016/j.scitotenv.2024.177294.
Fisher, R.A., 1925. Statistical Methods For Research Workers. Oliver and Boyd, Edinburgh, Scotland.
Ford, D.C., Williams, P.W., 2007. Karst Hydrogeology and Geomorphology. Wiley.
Frank, S., Goeppert, N., Goldscheider, N., 2018. Fluorescence-based multi-parameter approach to characterize dynamics of organic carbon, faecal bacteria, and particles at alpine karst springs. Sci. Total. Environ. 615, 1446–1459. https://doi.org/10.1016/j.scitotenv.2017.09.095.
Frank, S., Fahrmeier, N., Goeppert, N., Goldscheider, N., 2022. High-resolution multi-parameter monitoring of microbial water quality and particles at two alpine karst springs as a basis for an early-warning system. Hydrogeol. J. 30, 2285–2298. https://doi.org/10.1007/s10040-022-02556-8.
Frattini, P., Crosta, G., Carrara, A., 2010. Techniques for evaluating the performance of landslide susceptibility models. Eng. Geol. 111 (1–4), 62–72. https://doi.org/10.1016/j.enggeo.2009.12.004.
Freund, Y., Schapire, R.E., 1997. A decision-theoretic generalization of on-line learning and an application to boosting. J. Comput. Syst. Sci. 55 (1), 119–139. https://doi.org/10.1006/jcss.1997.1504.
Goldscheider, N., Drew, D., 2007. Methods in Karst Hydrogeology. Taylor & Francis.
Gorsevski, P.V., Gessler, P.E., Foltz, R.B., Elliot, W.J., 2006. Spatial prediction of landslide hazard using logistic regression model and ROC analysis. Trans. GIS. 10 (3), 395–415. https://doi.org/10.1111/j.1467-9671.2006.01004.x.
Grimmeisen, F., Riepl, D., Schmidt, S., Xanke, J., Goldscheider, N., 2018. Set-up of an early warning system for an improved raw water management of karst groundwater resources in the semi-arid side Wadis of the Jordan Valley. In: EGU General Assembly Conference Abstracts, 20, 16731. https://ui.adsabs.harvard.edu/abs/2018EGUGA..2016731G.
Haggerty, R., Sun, J., Yu, H., Li, Y., 2023. Application of machine learning in groundwater quality modeling—A comprehensive review. Water. Res. 229, 119745. https://doi.org/10.1016/j.watres.2023.119745.
Hanley, J.A., McNeil, B.J., 1983. A method of comparing the areas under receiver operating characteristic curves derived from the same cases. Radiology 148 (3), 839–843. https://doi.org/10.1148/radiology.148.3.6878708.
Henderson, R.K., Baker, A., Murphy, K.R., Hambly, A., Stuetz, R.M., Khan, S.J., 2009. Fluorescence as a potential monitoring tool for recycled water systems: a review. Water. Res. 43 (4), 863–881. https://doi.org/10.1016/j.watres.2008.11.027.
Hudson, N., Baker, A., Reynolds, D., 2007. Fluorescence analysis of dissolved organic matter in natural, waste and polluted waters: a review. River. Res. Appl. 23 (6), 631–649. https://doi.org/10.1002/rra.1005.
Huerta, I.I., Neira, D.A., Ortega, D.A., Varas, V., Godoy, J., Asín-Achá, R., 2022. Improving the state-of-the-art in the traveling salesman problem: an anytime automatic algorithm selection. Expert. Syst. Appl. 187, 115948. https://doi.org/10.1016/j.eswa.2021.115948.
Instituto Nacional de Estadística (INE), 2024. Censo De Población y Viviendas 2024. Instituto Nacional de Estadística, Madrid.
Katz, B.G., Eberts, S.M., Kauffman, L.J., 2011. Using Cl/Br ratios and other indicators to assess potential impacts on groundwater quality from septic systems: a review and examples from principal aquifers in the United States. J. Hydrol. 397 (1–2), 151–166. https://doi.org/10.1016/j.jhydrol.2010.11.017.
Liñán Baena, C., Andreo, B., Mudry, J., Carrasco, F., Durán, J.J., Jiménez, P., 2009. Groundwater temperature and electrical conductivity as tools to characterize flow patterns in carbonate aquifers: the Sierra de las Nieves karst aquifer, southern Spain. Hydrogeol. J. 17 (4), 843–853. https://doi.org/10.1007/s10040-008-0395-x.
Mahler, B.J., Lynch, F.L., 1999. Muddy waters: temporal variation in sediment discharging from a karst spring. J. Hydrol. 214 (1–4), 165–178. https://doi.org/10.1016/S0022-1694(98)00287-X.
Mahler, B.J., Personne, J.C., Lods, G.F., Drogue, C., 2000. Transport of free and particulate-associated bacteria in karst. J. Hydrol. 238 (3–4), 179–193. https://doi.org/10.1016/S0022-1694(00)00324-3.
Marsaud, B., 1997. Structure et fonctionnement de la zone noyée des karsts à partir des résultats expérimentaux (Structure and functioning of the saturated zone of karsts from experimental results). Doc. du BRGM 268. Editions de BRGM.
Mahlknecht, J., Torres-Martínez, J.A., Kumar, M., Mora, A., Kaown, D., Loge, F.J., 2023. Nitrate prediction in groundwater of data scarce regions: the futuristic fresh-water management outlook. Sci. Total. Environ. 905, 166863. https://doi.org/10.1016/j.scitotenv.2023.166863.
Martín-Algarra, A. (1987). Evolución geológica alpina del contacto entre las Zonas Internas y las Externas de la Cordillera Bética [Doctoral thesis, Universidad de Granada].
Martín-Rodríguez, J.F., Mudarra, M., De la Torre, B., Andreo, B., 2023. Towards a better understanding of time-lags in karst aquifers by combining hydrological analysis tools and dye tracer tests: application to a binary karst aquifer in southern Spain. J Hydrol 621, 129643. https://doi.org/10.1016/j.jhydrol.2023.129643.
Massei, N., Wang, H.Q., Dupont, J.P., Rodet, J., Laignel, B., 2003. Assessment of direct transfer and resuspension of particles during turbid floods at a karstic spring. J Hydrol 275 (1–2), 109–121. https://doi.org/10.1016/S0022-1694(03)00020-9.
McCulloch, W.S., Pitts, W., 1943. A logical calculus of the ideas immanent in nervous activity. Bull. Math. Biophys. 5 (4), 115–133. https://doi.org/10.1007/BF02478259.
McLachlan, G.J., 1992. Discriminant Analysis and Statistical Pattern Recognition. Wiley.
Moguerza, J.M., Muñoz, A., 2006. Support vector machines with applications. Stat. Sci. 21 (3), 322–336. https://doi.org/10.1214/088342306000000493.
Mohammadagha, M., 2025. Hyperparameter optimization strategies for tree-based machine learning models prediction: a comparative study of AdaBoost, decision trees, and random forest. SSRN Electron. J. https://doi.org/10.2139/ssrn.5226457.
Nettleton, D.F., Orriols-Puig, A., Fornells, A., 2010. A study of the effect of different types of noise on the precision of supervised learning techniques. Artif. Intell. Rev. 33 (4), 275–306. https://doi.org/10.1007/s10462-010-9156-z.
Nowicki, S., Lapworth, D., Ward, J., Thomson, P., Charles, K., 2019. Tryptophan-like fluorescence as a measure of microbial contamination risk in groundwater. Sci. Total. Environ. 646, 782–791. https://doi.org/10.1016/j.scitotenv.2018.07.327.
Olstadt, J., Schauer, J.J., Standridge, J., Kluender, S., 2007. A comparison of ten USEPA approved total coliform/E. coli tests. J. Water. Health 5 (2), 267–282. https://doi.org/10.2166/wh.2007.024.
Onyango, L.A., Quinn, C., Tng, K.H., Wood, J.G., Leslie, G., 2015. A study of failure events in drinking water systems as a basis for comparison and evaluation of the efficacy of potable reuse schemes. Env. Health Insights 9 (s3), EHI.S31749. https://doi.org/10.4137/EHI.S31749.
Pedregosa, F., Varoquaux, G., Gramfort, A., Michel, V., Thirion, B., Grisel, O., Blondel, M., Prettenhofer, P., Weiss, R., Dubourg, V., Vanderplas, J., Passos, A., Cournapeau, D., Brucher, M., Perrot, M., Duchesnay, É., 2011. Scikit-learn: machine learning in Python. J. Mach. Learn. Res. 12, 2825–2830.
Podgorski, J., Berg, M., 2020. Global threat of arsenic in groundwater. Science 368 (6494), 845–850. https://doi.org/10.1126/science.aba1510.
Podgorski, J., Berg, M., 2022. Global analysis and prediction of fluoride in groundwater. Nat. Commun. 13, 4232. https://doi.org/10.1038/s41467-022-31940-x.
Pras, A., Mamane, H., 2023. Nowcasting of fecal coliform presence using an artificial neural network. Environ. Pollut. 326, 121484. https://doi.org/10.1016/j.envpol.2023.121484.
Pronk, M., Goldscheider, N., Zopfi, J., 2007. Particle-size distribution as indicator for fecal bacteria contamination of drinking water from karst springs. Env. Sci. Technol 41 (24), 8421–8428. https://doi.org/10.1021/es071976f.
Quinlan, J.R., 1986. Induction of decision trees. Mach. Learn. 1 (1), 81–106. https://doi.org/10.1007/BF00116251.
Rashidi, H.H., Albahra, S., Robertson, S., Tran, N.K., Hu, B., 2023. Common statistical concepts in the supervised machine learning arena. Front. Oncol. 13, 1130229. https://doi.org/10.3389/fonc.2023.1130229.
Rasmussen, C.E., Williams, C.K.I., 2006. Gaussian Processes For Machine Learning. MIT Press.
Ravbar, N., Mulec, J., Mayaud, C., Blatnik, M., Kogovšek, B., Petrič, M., 2023. A comprehensive early warning system for karst water sources contamination risk: case study of the Unica springs, SW Slovenia. Sci. Total. Environ. 885, 163958. https://doi.org/10.1016/j.scitotenv.2023.163958.
RD 3/2023, 2023. Real Decreto-ley de 10 de enero, por el que se establecen los criterios técnico-sanitarios de la calidad del agua de consumo, su control y suministro. Bol. Of. Estado 9, 4253–4354.
Ryan, M., Meiman, J., 1996. An examination of short-term variations in water quality at a karst spring in Kentucky. Ground. Water. 34 (1), 23–30. https://doi.org/10.1111/j.1745-6584.1996.tb01861.x.
Singha, S., Pasupuleti, S., Singha, S.S., Singh, R., Kumar, S., 2021. Prediction of groundwater quality using efficient machine learning technique. Chemosphere 276, 130265. https://doi.org/10.1016/j.chemosphere.2021.130265.
Sorensen, J.P.R., Lapworth, D.J., Marchant, B.P., Nkhuwa, D.C.W., Pedley, S., Stuart, M. E., Bell, R.A., Chirwa, M., Kabika, J., Liemisa, M., Chibesa, M., 2015. In situ tryptophan-like fluorescence: a real-time indicator of faecal contamination in drinking water supplies. Water. Res. 81, 38–46. https://doi.org/10.1016/j.watres.2015.05.035.
Stadler, H., Klock, E., Skritek, P., Mach, R.L., Zerobin, W., Farnleitner, A.H., 2010. The spectral absorption coefficient at 254 nm as a real-time early warning proxy for detecting faecal pollution events at alpine karst water resources. Water. Sci. Technol. 62 (8), 1898–1906. https://doi.org/10.2166/wst.2010.500.
Stamenković, L.J., Mrazovac Kurilić, S., Presburger Ulniković, V., 2020. Prediction of nitrate concentration in Danube River water by using artificial neural networks. Water Suppl. 20 (6), 2119–2132. https://doi.org/10.2166/ws.2020.183.
Stevanović, Z., 2019. Karst waters in potable water supply: a global scale overview. Env. Earth Sci. 78, 662. https://doi.org/10.1007/s12665-019-8670-9.
Stevanovic, Z., Stevanović, A.M., 2021. Monitoring as the key factor for sustainable use and protection of groundwater in karst environments—An overview. Sustainability 13 (10), 5468. https://doi.org/10.3390/su13105468.
Storey, M.V., van der Gaag, B., Burns, B.P., 2011. Advances in on-line drinking water quality monitoring and early warning systems. Water. Res. 45 (2), 747–756. https://doi.org/10.1016/j.watres.2010.08.049.
Thompson, M.Y., Brandes, D., Kney, A.D., 2012. Using electronic conductivity and hardness data for rapid assessment of stream water quality. J. Env. Manage 104, 152–157. https://doi.org/10.1016/j.jenvman.2012.03.025.
U.S. Environmental Protection Agency, 2005. Technologies and Techniques For Early Warning Systems to Monitor and Evaluate Drinking Water quality: A state of the Art Review (EPA/600/R-05/156). U.S. Environmental Protection Agency, Washington, DC.
World Health Organization, 1997. Guidelines For Drinking-Water Quality, 2nd ed. WHO Press, Geneva, Switzerland.
World Health Organization, 2006. Guidelines For the Safe Use of wastewater, Excreta and Greywater in Agriculture and Aquaculture (Vols. 1–4). World Health Organization, Geneva, Switzerland.